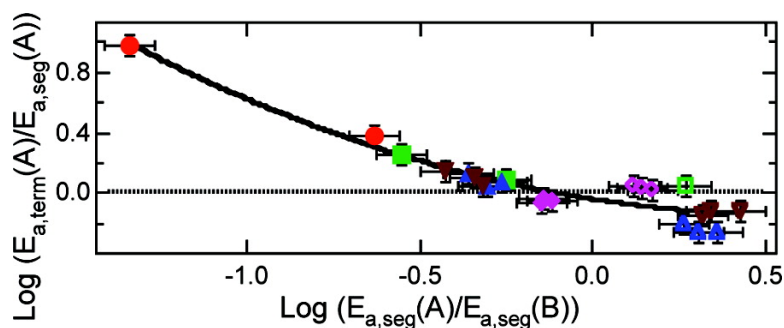


## Poly(ethylene oxide) Dynamics in Blends with Poly(vinyl acetate): Comparison of Segmental and Terminal Dynamics

Junshu Zhao, Liang Zhang, and M. D. Ediger

*Macromolecules*, 2008, 41 (21), 8030-8037 • DOI: 10.1021/ma8010526 • Publication Date (Web): 07 October 2008

Downloaded from <http://pubs.acs.org> on November 25, 2008



### More About This Article

Additional resources and features associated with this article are available within the HTML version:

- Supporting Information
- Access to high resolution figures
- Links to articles and content related to this article
- Copyright permission to reproduce figures and/or text from this article

[View the Full Text HTML](#)



# Poly(ethylene oxide) Dynamics in Blends with Poly(vinyl acetate): Comparison of Segmental and Terminal Dynamics

Junshu Zhao, Liang Zhang, and M. D. Ediger\*

Chemistry Department, University of Wisconsin—Madison, 1101 University Ave., Madison, Wisconsin 53706

Received May 9, 2008; Revised Manuscript Received July 28, 2008

**ABSTRACT:** Deuterium NMR at Larmor frequencies of 15.6 and 76.7 MHz was used to study the segmental dynamics of perdeuteriopoly(ethylene oxide) ( $d_4$ PEO) in miscible blends with poly(vinyl acetate) (PVAc). Blends with PEO compositions of 2% and 50% were studied. The segmental dynamics of PEO are 9 orders of magnitude faster than the PVAc segmental dynamics for a 2% PEO blend near the blend  $T_g$  and could be described by the Lodge–McLeish model with a self-concentration of 0.3. The segmental dynamics of PEO in blends with PVAc show a weaker temperature dependence than the terminal dynamics of PEO in the same blends. We also compare the segmental and terminal dynamics of components in several other miscible polymer blends. For the fast component in a blend, it is commonly observed that terminal relaxation has a stronger temperature dependence than segmental relaxation. This effect correlates with the difference between the  $T_g$  values for the pure components and also with the ratio of the activation energies of the segmental dynamics for the two components in the blend.

## Introduction

Understanding the relationship between segmental and terminal dynamics in a polymer system is of importance both scientifically and practically. Segmental dynamics characterize the conformational transitions of polymer chains, determining the glass transition temperature ( $T_g$ ) and the transport properties of small molecules in a polymer matrix. Terminal dynamics characterize the fluctuations of the end-to-end vectors of polymer chains and strongly influence rheology and chain diffusion. For pure homopolymers, the relationship between the two dynamic processes is well-studied. At temperatures well above  $T_g$  for a pure homopolymer, it is commonly observed that the ratio of the terminal relaxation time ( $\tau_1$ ) to the segmental relaxation time ( $\tau_{\text{seg}}$ ) is a constant.<sup>1,2</sup> This is consistent with the generally accepted view that segmental motion is the fundamental kinetic process that drives all other processes on longer length and time scales. The Rouse model,<sup>3</sup> which adopts a bead–spring model for a polymer chain, successfully reproduces this proportionality between dynamics at different length scales. This simple proportionality makes it easy to predict one dynamic process given the other and thus has practical significance.

Many applications of polymers involve tuning the overall dynamic properties of a material by blending different polymers together. Being able to predict the dynamics in polymer blends is of great importance. However, miscible polymer blends are complicated dynamic systems featuring anomalously broad DSC glass transitions<sup>4</sup> and the failure of time–temperature superposition.<sup>5</sup> Significant effort has recently been given to understanding how the segmental dynamics of each component changes upon blending. Components in a miscible polymer blend have distinct segmental dynamics.<sup>4,6</sup> Unlike miscible small molecule mixtures in which all the components move at similar rates, the segmental dynamics of a polymer in a miscible blend are biased to those of its pure homopolymer. This explains, at least qualitatively, the broad DSC glass transition and partially explains the failure of time–temperature superposition. The Lodge–McLeish (LM) model<sup>7</sup> is one approach that captures these features by considering the self-concentration effect (the enhanced local concentration due to chain connectivity). In some systems,<sup>8,9,12</sup> quantitative agreement has been found between the model predictions and experimental results.

In addition to understanding component segmental dynamics in miscible blends, it is necessary to understand the relationship between segmental and terminal dynamics for each component in order to predict the rheological properties of the blend.<sup>10,11</sup> While the idea of self-concentration indicates that the LM model is specifically applicable for segmental dynamics, it has also been used to describe<sup>12–15</sup> and predict<sup>10,11</sup> terminal dynamics in some cases. The use of the LM model in this way assumes that segmental and terminal relaxation processes for a given component in a miscible blend are tightly coupled and have the same temperature dependence. However, no systematic test of this assumption has yet been made. The literature indicates a range of behaviors among different miscible polymer blend systems. For polyisoprene/poly(vinyl ethylene) (PI/PVE),<sup>8</sup> a single self-concentration value can fit both the segmental and terminal dynamics of the PI component in blends with various compositions indicating that the two processes have the same temperature dependence. For poly(ethylene oxide)/poly(methyl methacrylate) (PEO/PMMA)<sup>5,16,17</sup> blends, however, a significant difference was found between the temperature dependence of terminal relaxation times and that of segmental relaxation times for the PEO component. For polyisoprene/polystyrene (PI/PS),<sup>18</sup> the component segmental dynamics have different temperature dependences while the component terminal dynamics have similar temperature dependences. For poly(vinyl ethylene)/poly(butylene oxide) (PVE/PBO),<sup>19</sup> a composition dependence of the separation between segmental and terminal relaxation times was reported for the PBO component, which indicates from a different perspective the failure of the Rouse proportionality relationship in this blend.

Here we report measurements of the segmental dynamics of deuterated poly(ethylene oxide) ( $d_4$ PEO) in miscible blends with poly(vinyl acetate) (PVAc) using  $^2\text{H}$  NMR. Blends containing 2% and 50%  $d_4$ PEO were studied. For each composition we performed  $^2\text{H}$  NMR  $T_1$  measurements in the miscible region at two different magnetic fields. Segmental correlation times were extracted using a modified Kohlrausch–Williams–Watts (mKWW) correlation function. The terminal dynamics of both PEO and PVAc components as well as the segmental dynamics of the PVAc component in blends with various compositions were previously studied by Urakawa et al.<sup>15</sup> We combine our results with the data of Urakawa et al. in order to study the relationship between the component segmental and terminal

\* To whom correspondence should be addressed.

dynamics. A second reason for studying a blend containing PEO is its relevance to PEO/PMMA blends whose unusual dynamic behavior has drawn considerable interest<sup>16,17,24,28,30–38</sup> and has sometimes been considered an atypical miscible blend system.<sup>36</sup> Studying another blend system with PEO as one component will help us better understand the behavior of PEO/PMMA blend.

We find that segmental and terminal dynamics of the PEO component in PVAc blends have increasingly different temperature dependences upon dilution of PEO. By comparing the data for a number of miscible blend systems, we find that terminal dynamics often have a stronger temperature dependence than the segmental dynamics for the fast component in a blend. Thus, the assumption that segmental and terminal processes have the same relationship in a blend as in a pure melt is often incorrect. We find that the ratio of the activation energies for segmental and terminal relaxation is correlated with the component  $T_g$  difference and the ratio of the activation energies of the segmental dynamics for the two components in the blend.

For the PEO/PVAc system, we find a large difference (up to 9 orders of magnitude) between the segmental relaxation times of the two components near the blend  $T_g$ , qualitatively similar to the difference of 12 orders of magnitude reported for the PEO/PMMA blend.<sup>16</sup> However, unlike the case of PEO/PMMA, the dynamics of PEO in blends with PVAc can be well described by the LM model with a  $\phi_{\text{self}}$  of 0.3, which is well within the range of  $\phi_{\text{self}}$  values commonly observed in miscible blend systems.<sup>12</sup> We discuss the anomalously large  $\phi_{\text{self}}$  value reported for the PEO component in blends with PMMA in terms of the experimental temperature range in that study. When the data for PEO in PEO/PMMA are fit over a restricted temperature range above the blend  $T_g$ , a  $\phi_{\text{self}}$  of 0.37 is found, indicating similarity between the behavior of PEO in PMMA and in PVAc.

## Experimental Section

**Materials.** Perdeuteriopoly(ethylene oxide) was purchased from Polymer Source (P2632-dEO). The  $d_4$ PEO has  $M_w = 1.6 \times 10^5$  g/mol with  $M_w/M_n$  equal to 1.07.  $T_g$  of PEO with similar molecular weight is previously reported to be 211 K.<sup>15</sup> Poly(vinyl acetate) with  $M_w = 1.2 \times 10^4$  g/mol and  $M_w/M_n = 1.77$  was kindly provided by Dr. Osamu Urakawa.  $T_g$  of this PVAc is 308 K.

**Blend Preparation.** The 2%  $d_4$ PEO/PVAc blend was prepared via freeze-drying with HPLC grade benzene. The 50%  $d_4$ PEO/PVAc blend was prepared by solvent casting from benzene solution. A detailed description of the preparation method can be found elsewhere.<sup>16,20</sup>

**$T_g$  and Miscibility.** The interaction parameter  $\chi$  for 2% deuterated PEO in PVAc was measured using small-angle neutron scattering by Huang<sup>41</sup> using polymers with similar molecular weights as those used in this study. Negative  $\chi$  values were extracted for the temperature range of 323–383 K. Extrapolating the  $\chi$  values to higher temperatures supports the miscibility of the blend up to 450 K (the highest temperature we studied). No direct neutron scattering data are available for the 50%  $d_4$ PEO/PVAc blend; however, a detailed study of the phase behavior of protonated PEO/PVAc blends has been published by Chen et al.<sup>21</sup> In their work, the phase diagrams of PEO ( $M_w = 4.62 \times 10^4$  g/mol) in blends with PVAc with varying molecular weights ( $M_w = 1.68 \times 10^4$ – $1.26 \times 10^5$  g/mol) were deduced both from DSC measurements and from a Sanchez–Lacombe lattice fluid (LF) theory calculation. Good agreement was found between the two methods, and both indicate a LCST phase behavior. If we assume that isotopic labeling has a negligible impact on the phase behavior of these polymer blends, the phase diagram of the PEO/PVAc blend used in our study can be estimated from Chen's study. For the 50% PEO/PVAc blend, we estimate the phase boundary to be around 390 K, and we set the upper temperature boundary for our measurement accordingly. PEO in the 50% blend crystallizes at around 335 K,<sup>15</sup> which sets the lower temperature limit for our measurement. For the NMR

measurements, if phase separation occurs, different  $T_1$  relaxation times are expected for different phases, in which case the decay of inverted magnetization should be nonexponential. For all our data, excellent single-exponential decays were observed, supporting the miscibility of the blends in the temperature range of our study.  $T_g$  of 2% PEO/PVAc blend was measured to be 305 K with differential scanning calorimetry by Urakawa et al.<sup>15</sup> Because of the crystallization of PEO,  $T_g$  cannot be accurately measured for the 50% PEO/PVAc blend.

**NMR Measurements.** As discussed in ref 15, dielectric relaxation measurement failed to detect the segmental dynamics of PEO component in blends with PVAc, indicating very fast PEO segmental dynamics. Since NMR detects segmental dynamics at higher frequencies than those typically used in the dielectric measurements, it is well-suited for studying the segmental dynamics of PEO in blends with PVAc.

Spin–lattice relaxation times  $T_1$  were measured using  $^2\text{H}$  NMR, and the standard inversion recovery ( $\pi - \tau - \pi/2$ ) pulse sequence.  $^2\text{H}$  NMR measurements were performed at two frequencies using two different NMR spectrometers: Varian Inova-500 NMR spectrometer (76.7 MHz) and Bruker DMX NMR spectrometer (15.6 MHz). Temperature was controlled to  $\pm 0.5$  K and calibrated to an uncertainty of  $\pm 2$  K using an ethylene glycol thermometer and melting point standards. Data were processed with line broadening equal to one-tenth the line width of the resonance peak, and the magnetization relaxation was fit with three parameters to obtain  $T_1$ . Intensities and peak areas were separately employed for the fit and yielded  $T_1$  values that agreed to within the experimental error of our measurements (6%). After exposure to high temperatures,  $T_1$  was reacquired at lower temperatures as a test for sample degradation. In all cases, the  $T_1$  measurements after exposure to high temperatures agreed with earlier measurements to within experimental error.

## Data Interpretation

**NMR Relaxation Equations.** Relaxation of the  $^2\text{H}$  nuclear spin is dominated by electric quadrupole coupling of deuterium nuclei. As shown below, the relaxation of the deuterium nuclei is related to the reorientation of the C–D bond.<sup>22,23</sup> The spin–lattice relaxation time of deuterium can be written as

$$\frac{1}{T_1} = \frac{3}{10} \pi^2 \left( \frac{e^2 q Q}{h} \right)^2 [J(\omega_D) + 4J(2\omega_D)] \quad (1)$$

Here  $\omega_D/2\pi$  is the Larmor frequency. The quadrupole coupling constant  $e^2 q Q/h$  was taken as  $155 \pm 3$  kHz (determined from the solid-state echo line shape at 183 K<sup>24</sup>) for  $d_4$ PEO deuterons. In eq 1,  $J(\omega)$  is the spectral density function, the Fourier transform of the orientation autocorrelation function  $G(t)$  for the C–D bond:

$$J(\omega) = \frac{1}{2} \int_{-\infty}^{\infty} G(t) e^{-i\omega t} dt \quad (2)$$

$G(t)$  is the function of our interest and can be written as

$$G(t) = \frac{3}{2} \langle \cos^2 \theta(t) \rangle - \frac{1}{2} \quad (3)$$

where  $\theta(t)$  is the angle of the C–D bond relative to its orientation at time  $t = 0$ .

**Correlation Function and Correlation Time.** We assume a modified Kohlrausch–Williams–Watts (mKWW) functional form for the orientation autocorrelation function. This functional form has been previously employed and been found to give excellent agreement with experimental data.<sup>25–27,40</sup>

$$G(t) = a_{\text{lib}} e^{-t/\tau_{\text{lib}}} + (1 - a_{\text{lib}}) e^{-(t/\tau_{\text{seg}})^\beta} \quad (4)$$

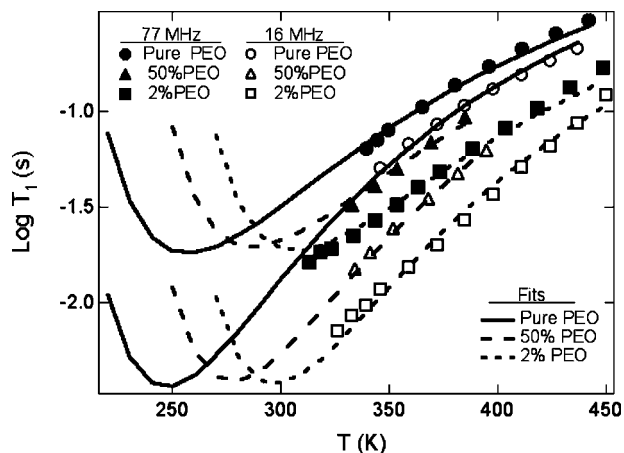


**Figure 1.**  $^2\text{H}$   $T_1$  values for pure  $d_4\text{PEO}$ , 2%  $d_4\text{PEO}$  in PVAc blend, and 50%  $d_4\text{PEO}$  in PVAc blend. Data were obtained at 16 and 77 MHz. Solid lines, dashed lines, and dotted lines are fits for pure PEO, 50% PEO, and 2% PEO, respectively. Fits are obtained by simultaneously fitting all the data to eqs 1–6 with  $B$  constrained to 354 K and  $a_{\text{lib}}$  constrained to 0.1. Fits are extended to lower temperatures to show the  $T_1$  minimum. Fit parameters are shown in Table 1.

**Table 1.** Fit Parameters for  $d_4\text{PEO}$  Dynamics in Blends with PVAc<sup>a</sup>

composition	2% $d_4\text{PEO}$	50% $d_4\text{PEO}$	pure $d_4\text{PEO}$
$\tau_{\infty}$ (ps)	0.021	0.015	0.020
$T_0$ (K)	230	212	180
$\beta$	0.233	0.225	0.243

<sup>a</sup>  $B$  constrained to 354 K, and  $a_{\text{lib}}$  constrained to 0.1.

This function indicates that C–D vector reorientation occurs via two mechanisms: librational and segmental motions. In this equation  $a_{\text{lib}}$  and  $\tau_{\text{lib}}$  are the amplitude and relaxation time for librational motion;  $\tau_{\text{lib}}$  is set to 1 ps in our fitting analysis, as the fit is insensitive to this value. The remaining two parameters in this equation,  $\tau_{\text{seg}}$  and  $\beta$ , describe a characteristic segmental relaxation time as well as the distribution of times associated with it. We assume that  $\tau_{\text{seg}}$  has Vogel–Tammann–Fulcher (VTF) temperature dependence:

$$\log\left(\frac{\tau_{\text{seg}}}{\tau_{\infty}}\right) = \frac{B}{T - T_0} \quad (5)$$

where  $\tau_{\infty}$ ,  $B$ , and  $T_0$  are constants for a given component in a particular blend. The correlation time for segmental dynamics  $\tau_{\text{seg,c}}$  is the time integral of the segmental portion of the correlation function

$$\tau_{\text{seg,c}} = \frac{\tau_{\text{seg}}}{\beta} \Gamma\left(\frac{1}{\beta}\right) \quad (6)$$

## Results

**$T_1$  Data and Fitting to the mKWW/VTF Function.** Figure 1 shows the measured  $^2\text{H}$   $T_1$  values for pure  $d_4\text{PEO}$  as well as 2% and 50%  $d_4\text{PEO}$  in PVAc blends. Data were acquired at  $^2\text{H}$  Larmor frequencies of 16 and 77 MHz. For pure PEO and the 50% PEO/PVAc blend, the  $T_1$  minimum was not reached due to the crystallization of PEO. For the 2% PEO/PVAc blend, acquisitions were done above the temperature at which the fwhm line width was 10 000 Hz, in which range the PEO component can be considered to be a liquid. The error bars for each data set are about the same size as the symbols.

Fitting of the deuterium  $T_1$  data was performed for pure PEO and both blends using eqs 1–6. Data for each composition were fit simultaneously for both fields. In this fitting procedure there

are five unknown parameters:  $a_{\text{lib}}$ ,  $\tau_{\infty}$ ,  $\beta$ ,  $B$ , and  $T_0$ . Because of the relatively small range of correlation times sampled in these measurements,  $B$  and  $T_0$  are highly correlated with each other. To be consistent with the fits for pure PEO in the study of PEO/PMMA system by Lutz et al.,<sup>16</sup>  $B$  was constrained to be 354 K for all compositions studied here. In addition, based on preliminary fits, the amplitude of libration was hardly affected by blending. Consequently for all compositions,  $a_{\text{lib}}$  was constrained to a value of 0.1, which is about the middle of all the  $a_{\text{lib}}$  values (0–0.4) that can fit the data. The fitted  $T_1$  curves for pure PEO, 50% PEO/PVAc, and 2% PEO/PVAc blends are shown in Figure 1 and give a good representation of the data; curves below the actual data acquisition temperatures are predictions from the fitting parameters to show the  $T_1$  minimum. Compared to unconstrained fits, adding the constraints described above did not significantly affect the fitting quality and did not have an impact on the  $\tau_{\text{seg,c}}$  values that we report below.

The parameters for the fits shown in Figure 1 are given in Table 1. Similar to the case of PEO/PMMA blends,<sup>16</sup> small  $\beta$  values are observed, indicating a broad distribution of relaxation times for  $d_4\text{PEO}$ .  $T_0$  increases monotonically with decreasing PEO concentration, indicating that the PEO dynamics slow down upon dilution with PVAc. Because of the broad distribution of relaxation times and the limited temperature range that did not include the  $T_1$  minimum, an array of fitting parameters provided comparable fits. When cooperatively adjusted, a wide range of  $B$  (over several hundred K) and  $T_0$  (over 100 K) can fit the data. Consequently, while the calculated correlation times are considered accurate, the values of the parameters should be considered with caution. In particular, allowing all other parameters to adjust freely, unconstrained fits gave values of  $\beta$  in the range of 0.22–0.28 for pure PEO, 0.22–0.25 for 2% PEO/PVAc, and 0.22–0.26 for 50% PEO/PVAc.

Our fitting procedure assumes that all the parameters are constants in the temperature range of our experiments. In a recent study of the dynamics of 20% PEO in a PVAc blend by quasi-elastic neutron scattering (QNS) experiments, Tyagi et al.<sup>42</sup> reported that the distribution of PEO relaxation times broadens at lower temperatures. To compare with their observations, we separately fitted our 2% PEO/PVAc data in low (<350 K), medium (350–400 K), and high (>400 K) temperature regions. The  $\beta$  values extracted for different temperature regions are consistent within 0.05, which indicates that for our experiments the distribution of relaxation times does not change significantly with temperature. It is possible that the difference between the NMR and neutron scattering results arises as a result of the different types of local motions probed by these techniques. Further study is required to better understand this issue.

As a check on our fitting procedure, a superposition of  $T_1$  data for different compositions is shown in Figure 2. One temperature shift is applied to each blend at both fields to yield the master curve; no vertical shifts are used here. The good superposition indicates that the dynamics of PEO in blends are approximately the same as those of pure PEO with only a temperature shift. For the 2% PEO/PVAc blend, the data were shifted 57 K to lower temperatures. This number is much smaller than the  $T_g$  difference of 97 K between the pure PEO and PVAc, indicating that the dynamics of the dilute PEO component are not slaved to its host. Thus, the segmental relaxation times for PEO and PVAc are distinct as discussed below.

**Correlation Times.** After fitting the  $T_1$  data as described above, we calculate the segmental correlation time  $\tau_{\text{seg,c}}$  of  $d_4\text{PEO}$  in the various blends using eq 6. Figure 3 presents the segmental correlation times of pure PEO as well as for PEO in the blends. An error bar of  $\pm 0.15$  to  $\pm 0.25$  decades is associated with the segmental correlation time for  $d_4\text{PEO}$  at the lowest

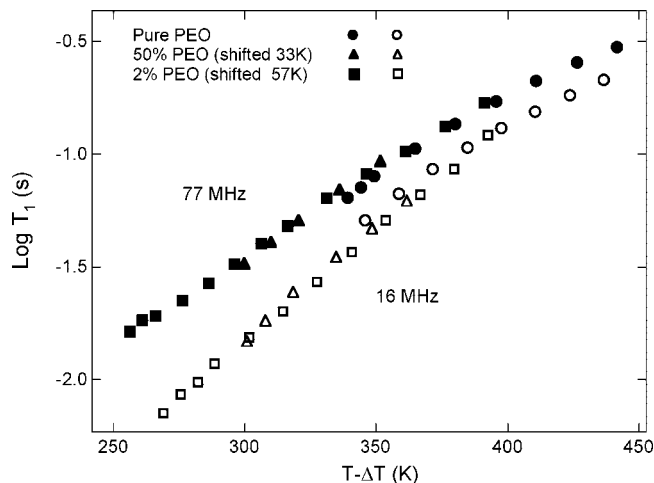


**Figure 2.** Superposition of  $^2\text{H}$   $T_1$  values for  $d_4\text{PEO}$  in blends and pure  $d_4\text{PEO}$ . Blend data are shifted to the pure PEO data using only temperature shifts. For each blend, a single temperature shift is used for data at both fields.

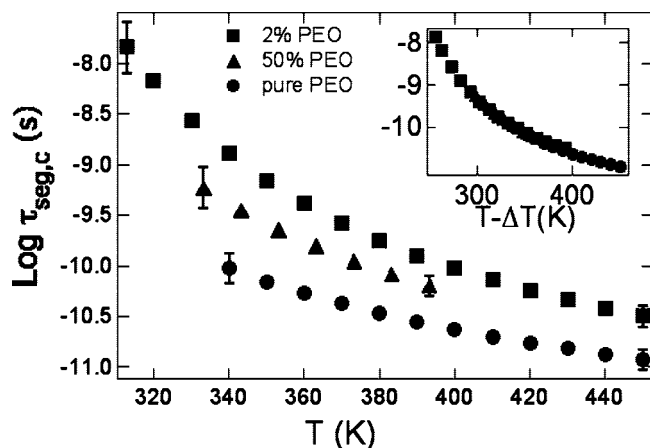


**Figure 3.** Segmental correlation times for pure  $d_4\text{PEO}$  and  $d_4\text{PEO}$  in blends with PVAc calculated from the fit parameters shown in Table 1. Representative error bars are shown. The inset shows a superposition of the three correlation time curves achieved by using temperature shifts. The shifts associated with the 2% PEO/PVAc blend and the 50% PEO/PVAc blend are 58 and 36 K, respectively.

temperatures; this error diminishes to  $\pm 0.1$  decades at the highest temperatures studied for all compositions. The inset shows the superposition of correlation times for all compositions. Similar to the raw data superposition shown in Figure 2, only temperature shifts are employed here. The quality of the superposition again argues that the segmental dynamics of the PEO component in these blends have approximately the same dynamics as pure PEO with a temperature offset. Shifts associated with 2% PEO/PVAc blend and 50% PEO/PVAc blend are 58 and 36 K, respectively. These numbers are in good agreement with the shifts for the raw  $T_1$  data shown in Figure 2, supporting the validity of the model used for data interpretation.

## Discussion

**Relationship between Segmental and Terminal Dynamics for PEO in PVAc.** A comparison between the temperature dependence of segmental and terminal dynamics of pure PEO as well as the PEO component in 2% and 50% PEO/PVAc blends is shown in Figure 4. Data representing terminal dynamics are viscoelastic shift factors measured by Urakawa et al.<sup>15</sup> for PEO/PVAc blends with comparable compositions

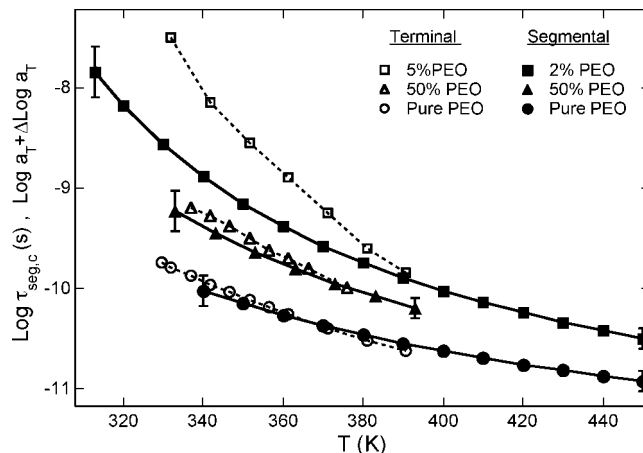


**Figure 4.** Comparison of temperature dependence of segmental and terminal dynamics of pure PEO and PEO in blends with PVAc. Terminal dynamics data are taken from ref 15 with vertical shifts applied. Solid and dashed lines are used to guide the eye.

as the blends used in our study. These shift factors are proportional to the terminal relaxation times ( $\tau_1$ ). To test the relationship between segmental and terminal dynamics for the PEO components in these blends, the shift factors are vertically shifted to the window of segmental correlation times. Since no terminal dynamics data have been reported for 2% PEO/PVAc blends, the terminal dynamics data for 5% PEO in PVAc are used here to compare with the segmental dynamics of 2% PEO in PVAc. As both compositions are in the dilute region, it is reasonable to compare these data directly. It can be seen from Figure 4 that over the temperature range studied segmental dynamics and terminal dynamics of pure PEO show similar temperature dependences. This observation agrees with the proportionality relationship discussed in the Introduction, which is true for most pure homopolymers well above  $T_g$ . However, as PEO is blended with PVAc, the temperature dependences of the two types of dynamics deviate. This deviation is quite significant for dilute PEO in PVAc; for dilute PEO chains at the low temperature end of our temperature range, the activation energy for terminal dynamics is 1.8 times higher than the activation energy for segmental dynamics.

Before we begin our discussion of the relationship between segmental and terminal dynamics in polymer blends, we briefly describe the behavior of pure homopolymers in the high-temperature region relevant to this paper. A recent study by Ding et al.<sup>1</sup> offers a good overview of this issue. For the six pure homopolymers investigated (*cis*-polyisoprene, polyoxybutylene, poly(propylene glycol), atactic polypropylene, polystyrene, and polycarbonate), they found that the ratio of terminal to segmental relaxation time is nearly constant at high temperatures, indicating similar temperature dependence of the segmental and terminal dynamics. At lower temperatures, however, when the segmental relaxation is slower than  $10^{-5}$ – $10^{-7}$  s, the ratio starts to drop and the dynamic behavior of pure homopolymers becomes more complicated. Similarly, work by Plazek<sup>2</sup> showed that thermorheological simplicity holds for PVAc in the temperature range from  $T_g + 25$  °C to  $T_g + 80$  °C but fails between  $T_g$  and  $T_g + 25$  °C. Thus, if the segmental and terminal dynamics of a given component in a polymer blend exhibit significantly different temperature dependences at temperatures where the segmental correlation times are less than  $10^{-7}$  s, this represents a unique feature of miscible blends.

**Relationship between Segmental and Terminal Dynamics in Other Miscible Blends.** We next consider the general relationship between component segmental and terminal dynamics combining the experimental results of PEO/PVAc blends

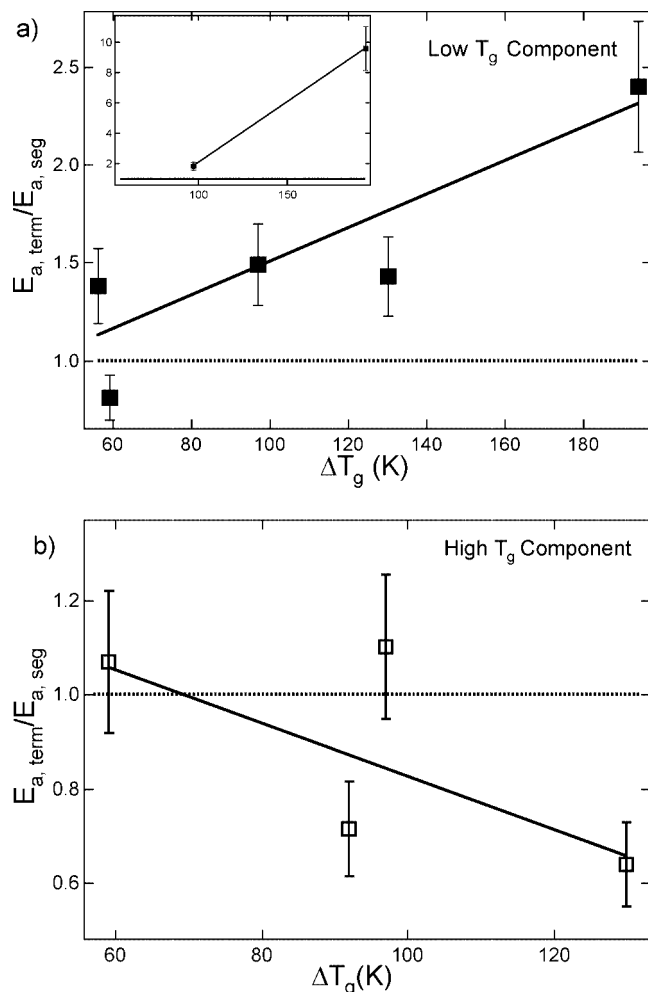


**Figure 5.** Ratio of the activation energy for terminal dynamics to the activation energy for segmental dynamics for the low- $T_g$  component (a) and the high- $T_g$  component (b) in various blends. Abscissas are the  $T_g$  difference between homopolymers. Dotted lines represent the behavior of homopolymer melts. The error bars shown reflect error propagation originating in uncertainties in the relaxation time data. (a) From left to right, data points are for PB in PVE,<sup>20</sup> PI in PVE,<sup>8</sup> PEO in PVAc,<sup>15</sup> PI in PS,<sup>18</sup> and PEO in PMMA.<sup>5,16</sup> The solid line is a guide to the eye. Compositions in the range of 20–30% low- $T_g$  polymer were chosen, except for PEO in PVAc where an average of 2% and 50% PEO was used. The inset shows the same plot but for dilute PEO in PVAc<sup>15</sup> and dilute PEO in PMMA.<sup>16,17</sup> (b) From left to right, data points are for PVE in PI, PVE in PB, PVAc in PEO, and PS in PI. Compositions in the range of 20–30% high- $T_g$  polymer, except for PVAc in PEO where 60% PVAc is used.

and literature information on other miscible blends.<sup>5,8,15–18,20</sup> We quantify this relationship by the ratio between the apparent activation energies for terminal ( $E_{a,term}$ ) and segmental dynamics ( $E_{a,seg}$ ), evaluated at the same temperature. A ratio of unity indicates the simple relationship between these quantities found in a polymer melt. In the remainder of this section, we will correlate the ratio  $E_{a,term}/E_{a,seg}$  with different blend properties in an effort to understand what controls the relationship between segmental and terminal dynamics.

Figure 5 shows the ratio  $E_{a,term}/E_{a,seg}$  for the low- $T_g$  components (a) and high- $T_g$  components (b) in different blends plotted against the  $T_g$  difference between their pure components.  $E_{a,term}/E_{a,seg}$  is taken at the lowest temperature at which both segmental and terminal dynamics data are available; more information is provided in Table S1 in the Supporting Information. The study of Ding et al.<sup>1</sup> shows that when segmental relaxation is slower than  $10^{-7}$  s, even for pure homopolymers, the temperature dependences of segmental and terminal dynamics can differ.

This effect does not contribute any ambiguity to our analysis since our comparisons are made for segmental correlation times of the components in the range of  $10^{-7}$ – $10^{-9}$  s. For all systems, similar compositions in the range of 20–30% low- $T_g$  component were chosen, except for PEO/PVAc blend. For the PEO/PVAc system, since the dynamics of blends with 20–30% PEO composition range were not studied, the average of this ratio for 2% PEO in PVAc and 50% PEO in PVAc is plotted in Figure 5a. For Figure 5b, due to the crystallization of PEO in blends with high PEO compositions,  $E_{a,term}/E_{a,seg}$  of the blend with lowest PVAc concentration studied<sup>15</sup> (60%) was plotted.

If the segmental and terminal dynamics of each component had the same temperature dependence in these polymer blends, all the symbols would fall on the horizontal line within their error bars. Figure 5a shows that for the low- $T_g$  component in a blend the ratio of the apparent activation energy for terminal dynamics to that for segmental dynamics is usually bigger than one. This ratio is even bigger for dilute blends as shown in the inset. Thus, blending with a slower component has a stronger effect on the terminal dynamics of the fast component than on the segmental dynamics. This observation is consistent with a recent work done by Niedzwiedz et al.<sup>28</sup> on the dynamics of PEO in blends with PMMA. They obtained the dynamics of the PEO component at short length scales with neutron backscattering and at a larger length scale with neutron spin-echo experiments. They found that the large length scale dynamics were much slower than the prediction of the Rouse model when the shorter scale dynamics were used as input. Niedzwiedz et al. explained this behavior by arguing that the larger scale dynamics of the fast component are not determined by the average local dynamics but rather are dominated by the lowest local mobilities.

The trend in Figure 5a indicates that the decoupling of the segmental and terminal dynamics of the fast component becomes more pronounced as the component  $T_g$  difference increases. For the PEO/PMMA blend, which has the largest component  $T_g$  difference, the deviation from proportionality is quite significant. Two other observations from the literature are consistent with this trend. Watanabe et al. reported anomalous broadening of the terminal dynamics of PI (fast) component in a blend with poly(4-*tert*-butylstyrene) (P4tBS).<sup>39</sup> For this blend, the components also have a large  $T_g$  difference (220 K). Watanabe et al.'s observation is consistent with Figure 5a in that a large component  $T_g$  difference is associated with a failure of simple models to describe the dynamics of the fast component in the blend. In their work published in 2006,<sup>19</sup> Hirose et al. tested the validity of Rouse model in miscible polymer blends from a different perspective. They found that the separation between segmental and terminal dynamics of the poly(butylene oxide) (PBO) (fast) component in blends with poly(vinyl ethylene) (PVE) varied with blend composition, indicating a failure of Rouse model in this blend. However, the variation ( $\sim 0.5$  decades) is relatively small, which given the small  $T_g$  difference (70 K) between the two components in that blend is consistent with Figure 5a.

For the high- $T_g$  component in a blend, it is not clear whether a corresponding correlation exists between the extent of deviation from Rouse model and the component  $T_g$  difference based on Figure 5b. The one clear outlier (PVAc in PEO/PVAc) was evaluated at a significantly different composition than the other systems, but we do not know whether this explains the deviation of this system from the trendline.

Another attempt to understand the distinct temperature dependences for segmental and terminal dynamics of components in miscible blends is motivated by a recent paper by Ngai.<sup>29</sup> Ngai related the different temperature dependences for segmental and terminal dynamics of the dilute PEO component

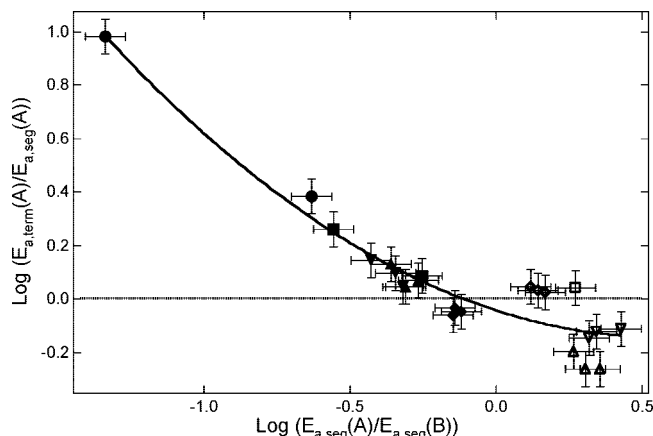


**Figure 6.** Logarithm of the ratio of the apparent activation energies for terminal and segmental dynamics of component A vs the logarithm of the ratio of apparent activation energies for segmental dynamics of A and B. Solid symbols are for the low- $T_g$  components, and open symbols are for the high- $T_g$  components. Circles are for PEO/PMMA<sup>5,16,17</sup> blends, squares for PEO/PVAc<sup>15</sup> blends, up triangles for PI/PS<sup>18</sup> blends, down triangles for PB/PVE<sup>20</sup> blends, and diamonds for PI/PVE<sup>8</sup> blends.

in blends with PMMA to the temperature dependences of the segmental dynamics of the two components. Ngai argued that terminal relaxation of PEO could not occur without some motion of the PMMA matrix. Thus, the terminal dynamics of PEO might be coupled to the segmental dynamics of PMMA in a way that the segmental dynamics of PEO is not.

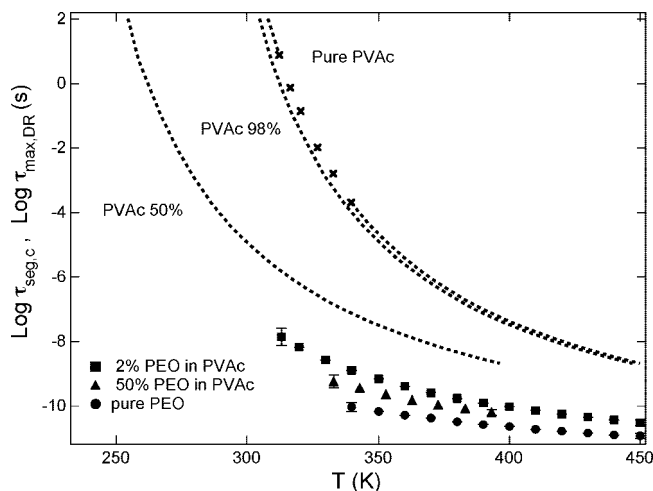
In Figure 6, we generalize this idea to other blends and compositions by plotting the ratio  $E_{a,term}(A)/E_{a,seg}(A)$  of one component A vs the ratio  $E_{a,seg}(A)/E_{a,seg}(B)$ . The plot is made on a double log scale, and the solid line is to guide the eye. For all the systems, these ratios are evaluated at the lowest temperature for which segmental and terminal dynamics data of A and the segmental dynamics data of B are all available and segmental dynamics of A is faster than  $10^{-7}$  s. Points with negative values of the abscissa all represent the low- $T_g$  component in these blends, and positive values are for the high- $T_g$  components. Table S2 in the Supporting Information provides additional details about the points plotted in Figure 6.

Figure 6 shows a reasonable correlation between  $E_{a,term}(A)/E_{a,seg}(A)$  and ratio of segmental activation energies for the two components. The miscible blend systems whose components exhibit segmental relaxation processes with quite different temperature dependences are also those systems for which the couplings between the segmental and terminal relaxation processes of a given component are the weakest. Thus, the terminal relaxation process of a component appears to depend upon the segmental relaxation processes of both components.

Figures 5 and 6 demonstrate two important points. They clearly show that segmental and terminal dynamics of a given component in a miscible blend often do not have the same temperature dependence. Furthermore, deviations from the simple behavior of homopolymer melts (dotted horizontal lines in Figures 5 and 6) are correlated with the dynamics in the blend, suggesting what factors need to be considered in modeling this behavior.

#### Distinct Segmental Dynamics in PEO/PVAc Blends.

Figure 7 summarizes the component segmental dynamics for 2% and 50% PEO/PVAc blends as well as the segmental dynamics of pure d<sub>4</sub>PEO and PVAc. The PEO dynamics are reproduced from Figure 3. The pure PVAc dynamics are from Urakawa's dielectric measurements.<sup>15</sup> The symbols are their experimental data after a small temperature shift to account for the 3 K  $T_g$  difference between the PVAc used in their study



**Figure 7.** Segmental dynamics of pure PEO, pure PVAc, and their component in blends. PEO component dynamics are calculated from fit parameters in Table 1. PVAc component dynamics are extracted from information in ref 15 as described in the text.

and ours. For the pure PVAc, the high-temperature part of the curve is obtained from the master curve presented by Urakawa.<sup>15</sup> From measurements on PVAc in blends with PEO (PVAc concentrations of 60–100%), Urakawa determined that a self-concentration value of 0.08 within the LM model reasonably reproduced data for the PVAc component. We have used this value to calculate the curves for 98% and 50% PVAc.

Figure 7 clearly shows that the PEO/PVAc miscible blend system exhibits distinct component dynamics. The ratio of PEO and PVAc segmental relaxation times becomes more pronounced upon the dilution of PEO. For the 2% PEO/PVAc blend, near the blend  $T_g$ , the segmental dynamics of dilute PEO is more than 9 orders of magnitude faster than the host PVAc. This is a remarkable difference, and the only system that has been reported to have a larger dynamic contrast is dilute PEO blended with PMMA.<sup>16</sup>

**LM Model Description of PEO Segmental Dynamics in PVAc.** The LM model<sup>7</sup> assumes that the chemical composition of the region within one cubic Kuhn length ( $l_K$ ) of a given polymer segment determines the mobility of that segment. This local concentration ( $\phi_{eff}$ ) is calculated by considering the bulk concentration ( $\phi_{self}$ ):

$$\phi_{eff} = \phi_{self} + (1 - \phi_{self})\phi \quad (7)$$

LM estimate the self-concentration  $\phi_{self}$  as

$$\phi_{self} = \frac{C_{\infty}M_0}{\kappa\rho N_{av}V} \quad (8)$$

Here  $C_{\infty}$  is the characteristic ratio,  $M_0$  is the repeat unit molar mass,  $\kappa$  is the number of backbone bonds per repeat unit,  $\rho$  is the density,  $N_{av}$  is Avogadro's number, and  $V = l_K^3$ .

In this model, polymer segments of a given type have an effective glass transition temperature that is different from the macroscopic blend  $T_g$  because  $\phi_{eff}$  differs from  $\phi$ . In our implementation of the LM model, we have used the Fox equation to calculate this effective  $T_g$

$$\frac{1}{T_g(\phi_{eff})} = \frac{\phi_{eff}}{T_{g,A}} + \frac{1 - \phi_{eff}}{T_{g,B}} \quad (9)$$

We predict segmental dynamics in the blend by correlating changes in  $T_{g,eff}$  with changes in  $T_0$

$$T_{0,i}(\phi) = T_{0,i} + [T_{g,i}(\phi) - T_{g,i}] \quad (10)$$

Thus, component dynamics in the blend can be predicted by applying a temperature shift to the segmental correlation times of the pure homopolymer.

Figure 8 shows the segmental relaxation times for PEO as a pure homopolymer and in the blend with PVAc, with the dotted lines showing the best fits to the LM model, obtained by treating  $\phi_{\text{self}}$  as a fitting parameter. The best fit is obtained when  $\phi_{\text{self}}$  is 0.30. The fits are reasonable given the error bars, indicating that the composition and temperature dependence of PEO segmental dynamics in PVAc blends can be described by the LM model. Although the  $\phi_{\text{self}}$  value obtained from fitting is larger than the value predicted by eq 8 (0.15), it is similar to the range of  $\phi_{\text{self}}$  values obtained by fitting data for many other miscible polymer blends.<sup>12</sup>

For these fits, the VTF curve describing the pure PEO dynamics is needed as an input. Because of the crystallization of PEO below 330 K, PEO dynamics cannot be measured at lower temperature, limiting the range of data available for fitting. The VTF parameters for PEO dynamics were determined by fitting the data along with the constraint  $\tau_{\text{seg,c}} = 100$  s at the PEO  $T_g$ .

**Comparison to Neutron Scattering Results.** As mentioned above, Tyagi et al. studied the dynamics of 20% PEO in a PVAc blend on a similar time scale ( $10^{-8}$ – $10^{-11}$  s) as our work using quasi-elastic neutron scattering.<sup>42</sup> On the basis of our NMR results, the segmental correlation times for PEO in this blend can be predicted by the LM model using our pure PEO dynamics and the extracted  $\phi_{\text{self}}$  value of 0.30. We compared the temperature dependence of the dynamics predicted from this method to the neutron scattering data. Depending upon the choice of wavevector, the temperature dependence of dynamics of the PEO component measured by neutron scattering experiment is weaker than or comparable to that of the predicted dynamics. For the PEO component in this 20% blend, the segmental dynamics measured by neutron scattering have a weaker temperature dependence than the terminal dynamics reported for this composition by Urakawa et al.<sup>15</sup> (see Figure S1 of the Supporting Information for a detailed comparison.) Thus, the neutron scattering data are broadly consistent with the principal conclusions of this paper.

**Comparison of Segmental Dynamics of PEO in PVAc and in PMMA.** Lutz et al.<sup>16</sup> reported that the segmental dynamics of PEO changes very little with a composition change from 3% to 30% in blends with poly(methyl methacrylate) (PMMA). For the 3% PEO blend near the blend  $T_g$ , the segmental dynamics of PEO are 12 orders of magnitude faster than the PMMA segmental dynamics. They reported that a fit of this data to the LM model gives a self-concentration value of 0.57 as compared to the value 0.15 predicted by the LM model. These unusual observations have drawn considerable interest.<sup>17,24,28,30–38</sup> Studying the dynamics of another system containing PEO can help us to better understand the unusual features of PEO/PMMA blends.

The results presented here for PEO in PVAc are qualitatively different than those reported for PEO in PMMA by Lutz et al., as indicated by the very different  $\phi_{\text{self}}$  values reported (0.30 vs 0.57). We reexamined the segmental dynamics data for PEO/PMMA system published by Lutz et al. For each composition, nearly half of the segmental dynamics data acquired for the PEO component were below the effective  $T_g$  of PMMA component in the blend. At such low temperatures, the PMMA component is moving so slowly that the equilibrium state cannot be reached in the time frame of the experiment. Since the LM model is an equilibrium model, it seems inappropriate to include data in this range in the fit to the LM model; it is well-known for

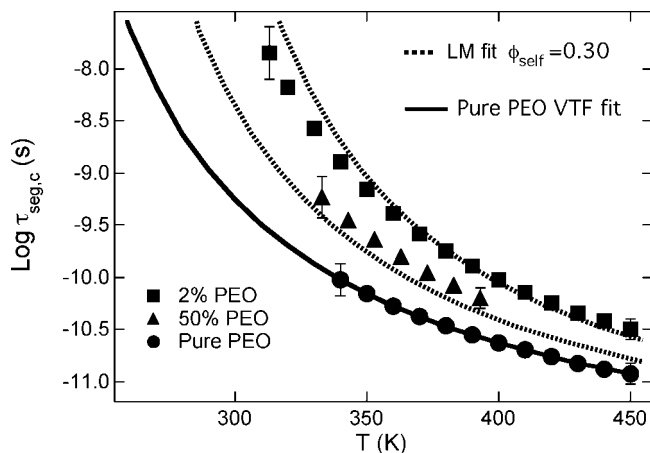


**Figure 8.** Lodge–McLeish fit of segmental dynamics for the PEO component in blends with PVAc. The solid curve represents pure PEO dynamics and is used as input to obtain the LM fits (dotted lines).

homopolymers that segmental dynamics in the glass have a different temperature dependence than dynamics above  $T_g$ .<sup>43</sup> In addition, quasi-elastic neutron scattering measurements<sup>32</sup> performed by Genix et al. indicate a significant qualitative change in the PEO dynamics in PMMA blends below the PMMA effective  $T_g$ . They attributed this observation to a “confinement effect”; i.e., the PEO chains need to move in a frozen PMMA matrix. With these considerations in mind, we refit the PEO/PMMA data from ref 16 using the LM model and using data only above the  $T_{g,\text{eff}}$  of PMMA in the blend. We obtained a  $\phi_{\text{self}}$  value of 0.37. This value is well within the range of  $\phi_{\text{self}}$  values that have been reported<sup>12</sup> and is close to the  $\phi_{\text{self}}$  value obtained here for PEO in blends with PVAc (0.3).

### Concluding Remarks

We carried out NMR  $T_1$  measurements to study the segmental dynamics of PEO in blends with PVAc with varying compositions. The results were compared with PEO terminal dynamics in the blends as well as the segmental dynamics of PEO in blends with PMMA. The above data along with literature results for PI/PVE, PEO/PMMA, PI/PS, and PB/PVE blends were used to examine the relationship between the component segmental and terminal dynamics in miscible polymer blends. There are four major findings in this work:

(1) The segmental dynamics of PEO in blends with PVAc are much faster than the segmental dynamics of the PVAc chains. For 2% PEO in PVAc, the PEO dynamics are about 9 orders of magnitude faster than the PVAc dynamics at the blend  $T_g$ . This behavior is qualitatively similar to that reported for the PEO/PMMA system.

(2) The segmental dynamics of dilute PEO chains in blends with PVAc has a considerably weaker temperature dependence (by a factor of  $\sim 1.8$ ) than the terminal dynamics of the same chains in the same blend.

(3) A comparison of literature data for several miscible blend systems indicates that, in contrast to the behavior of homopolymer melts, segmental and terminal relaxation times often have significantly different activation energies. For the low- $T_g$  component, the terminal dynamics usually have a stronger temperature dependence than the segmental dynamics. This behavior can be correlated with two blend properties: the  $T_g$  difference between components and the difference between the temperature dependence of the segmental dynamics of the two components in the blend.

(4) The segmental dynamics of PEO in blends with PVAc can be well-described by the Lodge–McLeish model with a  $\phi_{\text{self}}$  of 0.30. If only data above the blend  $T_g$  are used to fit the

PEO/PMMA system, a value of 0.37 is obtained, similar to that obtained for PEO/PVAc. Thus, it appears that these two systems are qualitatively similar.

**Acknowledgment.** This research was supported by the National Science Foundation through the Division of Material Research, Polymer Program (DMR-0355470). Measurements were performed at the Instrument Center of the Department of Chemistry, University of Wisconsin—Madison, supported by NSF CHE-9629688. We thank Charles Fry, Monika Ivancic, and Robert Shanks for their support. We thank Professor Osamu Urakawa for helpful discussions.

**Supporting Information Available:** Table S1 containing detailed information about the data plotted in Figure 5; Table S2 containing detailed information about the data plotted in Figure 6; Figure S1 comparing quasi-elastic neutron scattering results<sup>42</sup> to terminal dynamics data for 20% PEO in PVAc. This material is available free of charge via the Internet at <http://pubs.acs.org>.

## References and Notes

- Ding, Y. F.; Sokolov, A. P. *Macromolecules* **2006**, *39*, 3322–3326.
- Plazek, D. J. *J. Polym. Sci., Polym. Phys. Ed.* **1982**, *20*, 729–742.
- Rouse, P. E., Jr. *J. Chem. Phys.* **1953**, *21*, 1272–1280.
- Chung, G. C.; Kornfield, J. A.; Smith, S. D. *Macromolecules* **1994**, *27*, 5729–5741.
- Colby, R. H. *Polymer* **1989**, *30*, 1275–1278.
- Chin, Y. H.; Inglefield, P. T.; Jones, A. A. *Macromolecules* **1993**, *26*, 5372–5378.
- Lodge, T. P.; McLeish, T. C. B. *Macromolecules* **2000**, *33*, 5278–5284.
- Haley, J. C.; Lodge, T. P.; He, Y. Y.; Ediger, M. D.; von Meerwall, E. D.; Mijovic, J. *Macromolecules* **2003**, *36*, 6142–6151.
- Lutz, T. R.; He, Y. Y.; Ediger, M. D. *Macromolecules* **2005**, *38*, 9826–9835.
- Haley, J. C.; Lodge, T. R. *J. Rheol.* **2005**, *49*, 1277–1302.
- Pathak, J. A.; Kumar, S. K.; Colby, R. H. *Macromolecules* **2004**, *37*, 6994–7000.
- He, Y. Y.; Lutz, T. R.; Ediger, M. D. *J. Chem. Phys.* **2003**, *119*, 9956–9965.
- Hirose, Y.; Urakawa, O.; Adachi, K. *Macromolecules* **2003**, *36*, 3699–3708.
- Es-Haghi, S. S.; Yousefi, A. A.; Oromiehie, A. *J. Polym. Sci., Part B: Polym. Phys.* **2007**, *45*, 2860–2870.
- Urakawa, O.; Ujii, T.; Adachi, K. *J. Non-Cryst. Solids* **2006**, *352*, 5042–5049.
- Lutz, T. R.; He, Y. Y.; Ediger, M. D.; Cao, H. H.; Lin, G. X.; Jones, A. A. *Macromolecules* **2003**, *36*, 1724–1730.
- Haley, J. C.; Lodge, T. P. *J. Chem. Phys.* **2005**, *122*, 234914.
- He, Y. Y.; Lutz, T. R.; Ediger, M. D.; Pitsikalis, M.; Hadjichristidis, N.; von Meerwall, E. A. *Macromolecules* **2005**, *38*, 6216–6226.
- Hirose, Y.; Adachi, K. *Macromolecules* **2006**, *39*, 1779–1789.
- He, Y. Y.; Lutz, T. R.; Ediger, M. D. *Macromolecules* **2004**, *37*, 9889–9898.
- Chen, X.; An, L. J.; Li, L. X.; Yin, J. H.; Sun, Z. Y. *Macromolecules* **1999**, *32*, 5905–5910.
- Zhu, W.; Ediger, M. D. *Macromolecules* **1995**, *28*, 7549–7557.
- Bovey, F. A. *NMR of Polymers*; Academic Press: San Diego, 1996.
- Cao, H. H.; Lin, G. X.; Jones, A. A. *J. Polym. Sci., Part B: Polym. Phys.* **2005**, *43*, 2433–2444.
- Min, B. C.; Qiu, X. H.; Ediger, M. D.; Pitsikalis, M.; Hadjichristidis, N. *Macromolecules* **2001**, *34*, 4466–4475.
- Bandis, A.; Wen, W. Y.; Jones, E. B.; Kaskan, P.; Zhu, Y.; Jones, A. A.; Inglefield, P. T.; Bendler, J. T. *J. Polym. Sci., Part B: Polym. Phys.* **1994**, *32*, 1707–1717.
- Qiu, X. H.; Moe, N. E.; Ediger, M. D.; Fetters, L. J. *J. Chem. Phys.* **2000**, *113*, 2918–2926.
- Niedzwiedz, K.; Wischewski, A.; Monkenbusch, M.; Richter, D.; Genix, A. C.; Arbe, A.; Colmenero, J.; Strauch, M.; Straube, E. *Phys. Rev. Lett.* **2007**, *98*, 168301.
- Ngai, K. L. *J. Non-Cryst. Solids* **2007**, *353*, 709–718.
- Cao, H. H.; Lin, G. X.; Jones, A. A. *J. Polym. Sci., Part B: Polym. Phys.* **2004**, *42*, 1053–1067.
- Farago, B.; Chen, C. X.; Maranas, J. K.; Kamath, S.; Colby, R. H.; Pasquale, A. J.; Long, T. E. *Phys. Rev. E* **2005**, *72*, 031809.
- Genix, A. C.; Arbe, A.; Alvarez, F.; Colmenero, J.; Willner, L.; Richter, D. *Phys. Rev. E* **2005**, *72*, 031808.
- Jin, X.; Zhang, S. H.; Runt, J. *Macromolecules* **2004**, *37*, 8110–8115.
- Liu, J. H.; Sakai, V. G.; Maranas, J. K. *Macromolecules* **2006**, *39*, 2866–2874.
- Lodge, T. P.; Wood, E. R.; Haley, J. C. *J. Polym. Sci., Part B: Polym. Phys.* **2006**, *44*, 756–763.
- Maranas, J. K. *Curr. Opin. Colloid Interface Sci.* **2007**, *12*, 29–42.
- Ngai, K. L.; Roland, C. M. *Macromolecules* **2004**, *37*, 2817–2822.
- Sakai, V. G.; Chen, C. X.; Maranas, J. K.; Chowdhuri, Z. *Macromolecules* **2004**, *37*, 9975–9983.
- Watanabe, H.; Matsumiya, Y.; Takada, J.; Sasaki, H.; Matsushima, Y.; Kuriyama, A.; Inoue, T.; Ahn, K. H.; Yu, W.; Krishnamoorti, R. *Macromolecules* **2007**, *40*, 5389–5399.
- He, Y. Y.; Lutz, T. R.; Ediger, M. D.; Ayyagari, C.; Bedrov, D.; Smith, G. D. *Macromolecules* **2004**, *37*, 5032–5039.
- Huang, C. I. *J. Polym. Res.* **2001**, *8*, 219–224.
- Tyagi, M.; Arbe, A.; Colmenero, J.; Frick, B.; Stewart, J. R. *Macromolecules* **2006**, *39*, 3007–3018.
- Schlosser, E.; Schonhals, A. *Polymer* **1991**, *32*, 2135–2140.

MA8010526